ISSN 0015-4628, Fluid Dynamics, 2022, Vol. 57, No. 1, pp. 1–11. © Pleiades Publishing, Ltd., 2022.
Russian Text © The Author(s), 2022, published in Izvestiya RAN. Mekhanika Zhidkosti i Gaza, 2022, Vol. 57, No. 1, pp. 3–13.

Acoustic Streaming Induced by Wall Oscillations of a Plane Rectangular Resonator

D. A. Gubaidullin[a],*, P. P. Osipov[a],, and R. R. Nasyrov[a],*****

[a] *Kazan Scientific Center of the Russian Academy of Sciences, Institute of Mechanics and Engineering, Kazan, 420111 Russia*

**e-mail: gubaidullin@imm.knc.ru*

***e-mail: petro300@rambler.ru*

****e-mail: nasyrov.ravil@bk.ru*

Received March 30, 2021; revised September 17, 2021; accepted September 21, 2021

Abstract—We consider the flow of a viscous compressible gas in a closed rectangular resonator induced by harmonic oscillations of its boundary on the first resonance frequency. The method of successive approximations is used to study the two-dimensional acoustic streaming in a resonator of arbitrary width. The existence of an acoustic streaming in the form of four Rayleigh vortices and four Schlichting vortices is revealed. The similarity between the acoustic streamings occurring in the cases of horizontal harmonic oscillations of an enclosure and oscillations of a resonator wall is shown, which indicates a weak influence of the means of standing wave generation on the acoustic streaming pattern. It is found that as the channel width decreases, the Schlichting vortex dimensions increase compared with those of Rayleigh vortices. When the channel width is less than six thicknesses of the acoustic boundary layer, the Rayleigh vortices disappear and only the Schlichting vortices remain. It is established that in the case of an oscillating enclosure the centers of the Rayleigh and Schlichting vortices lie in the same cross-section, while in the case of the resonator with an oscillating boundary the centers of the Schlichting vortices are displaced toward the vertical walls.

Keywords: acoustic streaming, resonators, Rayleigh vortices, Schlichting vortices

DOI: 10.1134/S0015462822010050

In wave fields of a viscous fluid acoustic streamings can be formed under certain conditions. The problem of the onset of an acoustic streaming produced by a plane standing wave in a two-dimensional channel of arbitrary width was first analytically investigated in [1]. In [2, 3] different modifications of the solution [1] were proposed but emphasis was placed on the flow outside the boundary layer [3, 4]. As shown in [5], Schlichting vortices arise inside the boundary layer, the direction of their rotation being opposite to that of the external Rayleigh vortices. A theoretical and numerical analysis of the acoustic streaming produced by a standing wave along an impermeable wall in a semi-infinite region was made in [6–8].

In [9] an analytical solution of the reduced Navier—Stokes equations was obtained in a noninertial reference frame fitted to a rectangular vibrating enclosure and an acoustic streaming occurring in a one-dimensional standing pressure wave was calculated. In [10] an acoustic streaming in a fixed two-dimensional rectangular resonator was studied numerically on the basis of the complete Navier—Stokes equations for a compressible viscous gas in the case of harmonic oscillations of its left boundary. It was shown that an acoustic streaming is formed in the resonator in the form of secondary Schlichting and Rayleigh vortices. The acoustic streaming velocity profiles obtained on the basis of the analytical solution of the reduced Navier—Stokes equations [9] and the numerical solution of the complete equations [10] were compared and their good agreement was established. Despite the good agreement of the results of those studies, we note that they deal with the boundary value problems with different boundary conditions and equations. For this reason, the purpose of this study is to obtain an analytical solution of the reduced Navier—Stokes equations for the boundary conditions used in [10].

1. FORMULATION OF THE PROBLEM

We consider a closed rectangular resonator, $L = 2x_0$ in length, occupying the spatial region $-x_0 \le x \le x_0$, $-y_0 \le y \le y_0$ (Fig. 1). An acoustic streaming in the resonator is excited by oscillations of its

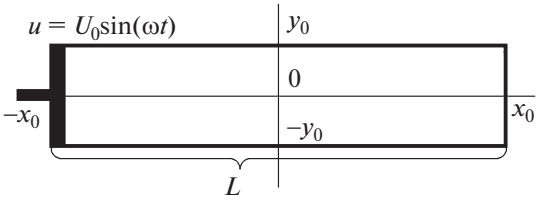

Fig. 1. Rectangular resonator.

left boundary. Following [9], the equation of continuity and the reduced Navier—Stokes equations can be written in the form:

$$\frac{\partial \rho}{\partial t} + \frac{\partial \rho u}{\partial x} + \frac{\partial \rho v}{\partial y} = 0,$$
$$\rho\left(\frac{\partial u}{\partial t} + u\frac{\partial u}{\partial x} + v\frac{\partial u}{\partial y}\right) = -\frac{\partial p}{\partial x} + \mu\frac{\partial^2 u}{\partial y^2}, \tag{1.1}$$
$$\frac{\partial p}{\partial y} = 0.$$

This system of three equations relates four quantities, namely, ρ, p, u, and v. To close it, the Poisson adiabat is used: $\rho/\rho_0 = (p/p_0)^{1/\gamma}$.

We note that here the momentum equation transverse to the channel is replaced by the condition of zero transverse pressure gradient, the transverse velocity component being determined from the continuity equation. This approach is substantiated in detail in [11], where the parameter of the smallness order $\eta = y_0/L$ was introduced and the following estimates were obtained

$$\frac{v}{u} = O(\eta), \quad \frac{\partial p/\partial y}{\partial p/\partial x} = O(\eta),$$

which indicate that in long narrow channels the fluid flow and the pressure gradients are directed mainly along the x axis.

We will then consider the periodic solution of Eq. (1.1) under the boundary conditions

$$\frac{1}{2y_0}\int_{-y_0}^{y_0} u(-x_0, y, t)dy = U_0 e^{i\omega t},$$
$$u(x_0, y, t) = 0, \tag{1.2}$$
$$u(x, -y_0, t) = 0, \quad v(x, -y_0, t) = 0,$$
$$u(x, y_0, t) = 0, \quad v(x, y_0, t) = 0.$$

2. METHOD OF SUCCESSIVE APPROXIMATIONS

Problem (1.1), (1.2) can be solved using the method of successive approximations in the form of the sum of disturbances of the first and second order of smallness [12]:

$$\rho = \rho_0 + \rho_1 + \rho_2, \quad p = p_0 + p_1 + p_2, \quad \mathbf{u} = \mathbf{u}_1 + \mathbf{u}_2.$$

For a polytropic gas, accurate to the third-order quantities we can write the expansion

$$p = p_0 + c_0^2(\rho - \rho_0) + \frac{(\gamma-1)c_0^2}{2\rho_0}(\rho - \rho_0)^2 = p_0 + c_0^2\rho_1 + \frac{(\gamma-1)c_0^2}{2\rho_0}\rho_1^2,$$

whence it follows that

$$p_1 = c_0^2\rho_1, \quad p_2 = \frac{(\gamma-1)c_0^2}{2\rho_0}\rho_1^2 + \rho_2 c_0^2 = \frac{\gamma-1}{2\rho_0 c_0^2}p_1^2 + \rho_2 c_0^2.$$

Accurate to the third-order small quantities, system (1.1) takes the form:

$$\frac{\partial(\rho_1+\rho_2)}{\partial t}+\frac{\partial(\rho_0+\rho_1+\rho_2)(u_1+u_2)}{\partial x}+\frac{\partial(\rho_0+\rho_1+\rho_2)(v_1+v_2)}{\partial y}=0,$$
$$(\rho_0+\rho_1+\rho_2)\left(\frac{\partial(u_1+u_2)}{\partial t}+(u_1+u_2)\frac{\partial(u_1+u_2)}{\partial x}+(v_1+v_2)\frac{\partial(u_1+u_2)}{\partial y}\right)$$
$$=-\frac{\partial(p_1+p_2)}{\partial x}+\mu\frac{\partial^2(u_1+u_2)}{\partial y^2}, \tag{2.1}$$
$$\frac{\partial(p_1+p_2)}{\partial y}=0.$$

2.1. First Approximation

For disturbances of the first order of smallness from Eq. (2.1) we can write the system

$$\frac{\partial\rho_1}{\partial t}+\rho_0\left(\frac{\partial u_1}{\partial x}+\frac{\partial v_1}{\partial y}\right)=0,\quad \rho_0\frac{\partial u_1}{\partial t}-\mu\frac{\partial^2 u_1}{\partial y^2}+\frac{\partial p_1}{\partial x}=0,\quad \frac{\partial p_1}{\partial y}=0,\quad p_1=\rho_1 c_0^2.$$

The solution of this system is sought in the complex form:

$$u_1=\mathrm{Im}[\tilde{u}_1 e^{i\omega t}],\quad v_1=\mathrm{Im}[\tilde{v}_1 e^{i\omega t}],\quad p_1=\mathrm{Im}[\tilde{p}_1 e^{i\omega t}] \tag{2.2}$$

under the boundary conditions (1.2).

Introducing complex amplitudes brings the first-approximation solution into the form:

$$\tilde{u}_1=u_0(x)Y_x(y),\quad \tilde{v}_1=-fy_0\frac{du_0}{dx}(x)Y_y(y),\quad \tilde{p}_1=-(1-f)\frac{\rho_0 c_0^2}{i\omega}\frac{du_0}{dx},$$

where

$$u_0(x)=\frac{0.5U_0}{1-f}\left(\frac{\cosh\alpha x}{\cosh\alpha x_0}-\frac{\sinh\alpha x}{\sinh\alpha x_0}\right),\quad Y_x(y)=1-\frac{\cosh\beta y}{\cosh\beta y_0},\quad Y_y(y)=\frac{y}{y_0}-\frac{\sinh\beta y}{\sinh\beta y_0},$$
$$\alpha=\frac{i\omega/c_0}{\sqrt{1-f}},\quad f=\frac{\tanh\beta y_0}{\beta y_0},\quad \beta=\frac{1+i}{\delta},\quad \delta=\sqrt{\frac{2\nu}{\omega}}.$$

2.2. Second Approximation and Acoustic Streaming

Separating out second-order disturbances from (2.1) yields the system

$$\frac{\partial\rho_2}{\partial t}+\rho_0\left(\frac{\partial u_2}{\partial x}+\frac{\partial v_2}{\partial y}\right)=-\left(\frac{\partial\rho_1 u_1}{\partial x}+\frac{\partial\rho_1 v_1}{\partial y}\right),$$
$$\rho_0\frac{\partial u_2}{\partial t}-\mu\frac{\partial^2 u_2}{\partial y^2}+\frac{\partial p_2}{\partial x}=-\frac{\partial\rho_1 u_1}{\partial t}-\rho_0\left(\frac{\partial u_1^2}{\partial x}+\frac{\partial u_1 v_1}{\partial y}\right), \tag{2.3}$$
$$\frac{\partial p_2}{\partial y}=0.$$

Averaging system (2.3) over a period leads to the system

$$\frac{\partial\overline{\rho_0 u_2+\rho_1 u_1}}{\partial x}+\frac{\partial\overline{\rho_0 v_2+\rho_1 v_1}}{\partial y}=0,$$
$$\mu\frac{\partial^2\overline{u}_2}{\partial y^2}-\frac{\partial\overline{p}_2}{\partial x}=\rho_0\left(\frac{\partial\overline{u_1^2}}{\partial x}+\frac{\partial\overline{u_1 v_1}}{\partial y}\right), \tag{2.4}$$
$$\frac{\partial\overline{p}_2}{\partial y}=0.$$

The second equation can be represented in the form:

$$\mu\frac{\partial^2\overline{u}_2}{\partial y^2} = \frac{d\overline{p}_2}{dx} - F(x,y), \tag{2.5}$$

where

$$F(x,y) = -\rho_0\left(\frac{\partial\overline{u_1^2}}{\partial x} + \frac{\partial\overline{u_1v_1}}{\partial y}\right). \tag{2.6}$$

Using in Eq. (2.6) the relation between the period-average product of two harmonics and their complex amplitudes $\overline{u_1v_1} = 0.5\mathrm{Re}[\tilde{u}_1\tilde{v}_1^*]$, $\overline{u_1^2} = 0.5\mathrm{Re}[\tilde{u}_1\tilde{u}_1^*]$ we can write

$$\frac{F(x,y)}{\mu} = -\frac{\rho_0}{2\mu}\mathrm{Re}\left[\frac{\partial(\tilde{u}_1\tilde{u}_1^*)}{\partial x} + \frac{\partial(\tilde{u}_1\tilde{v}_1^*)}{\partial y}\right] = -V_0\mathrm{Re}\left[G(x)\left(\frac{Y_xY_x^*}{\delta^2} - \frac{y_0f^*}{2\delta^2}\frac{d(Y_xY_y^*)}{dy}\right)\right], \tag{2.7}$$

where

$$V_0 = \frac{|U_0|^2\,\delta^2}{x_0\nu} = \frac{2|U_0|^2}{x_0\omega}, \quad G(x) = \frac{x_0}{|U_0|^2}\tilde{u}_0\frac{d\tilde{u}_0^*}{dx}.$$

The double integration of Eq. (2.5) with respect to y leads to the equation

$$\mu\overline{u}_2 = \frac{y^2}{2}\frac{d\overline{p}_2}{dx} - \int\int F(x,y)dydy + \mu C_1(x)y + \mu C_0(x),$$

where $C_0(x)$ and $C_1(x)$ are the integration constants determined from the boundary conditions.

Due to the problem symmetry, $\overline{u}_2$ is an even function of y, whence $C_1(x) = 0$ and, finally

$$\overline{u}_2 = \frac{y^2}{2\mu}\frac{d\overline{p}_2}{dx} - \frac{1}{\mu}\int\int F(x,y)dydy + C_0(x).$$

The double integral of Eq. (2.7) can be written in the form:

$$\frac{1}{\mu}\int\int F(x,y)dydy = -V_0\mathrm{Re}\left[G(x)\left(H_1 + iH_2\right)\right], \tag{2.8}$$

where

$$H_1 = \frac{1}{\delta^2}\left(\iint Y_xY_x^*dydy - \frac{y^2}{2}\right), \quad H_2 = \frac{1}{\delta^2}\left(\int Y_xY_y^*dy + \frac{if^*y^2}{4}\right)$$

Using the relations

$$\beta^2 + \beta^{*2} = 0, \quad \beta^2 - \beta^{*2} = \frac{4i}{\delta^2}, \quad \mathrm{Re}[iz] = -\mathrm{Im}[z], \quad \sinh iz = i\sin z, \quad \cosh iz = \cos z,$$

we obtain

$$H_1 = \frac{\cosh(2y/\delta) - \cos(2y/\delta)}{8|\cosh\beta y_0|^2} - \mathrm{Im}\frac{\cosh\beta y}{\cosh\beta y_0}$$

$$H_2 = f^*\frac{\cosh\beta y - \beta y\sinh\beta y}{4\cosh\beta y_0} + \frac{1}{4}\frac{\cosh\beta^* y}{\cosh\beta^* y_0} - \frac{\cosh(2y/\delta) + i\cos(2y/\delta)}{8\beta\delta|\cosh\beta y_0|^2}.$$

For the mean velocity we obtain

$$\overline{u}_2 = V(G,y) + C_2(x)y^2 + \overline{u}_2(x,0),$$

where $V(G,y) = V_0\mathrm{Re}[G(H_1(y) + iH_2(y))]$, while $C_2(x)$ includes the coefficients of the terms proportional to y^2 excluded from Eq. (2.8)

$$C_2(x) = \frac{1}{2\mu}\left(\frac{d\overline{p}_2}{dx} + \frac{\rho_0 \left|U_0^2\right|}{2x_0}\mathrm{Re}\left[(2 - f^*)G(x)\right]\right).$$

This equation is necessary for determining the pressure $\overline{p}_2$.

2.3. Mean Bulk Velocity

This quantity is determined as follows:

$$\overline{\mathbf{u}}_2^M = \frac{\overline{\rho\mathbf{u}}}{\overline{\rho}} \approx \frac{\overline{(\rho_0 + \rho_1)(\mathbf{u}_1 + \mathbf{u}_2)}}{\overline{\rho_0 + \rho_1}} \approx \overline{\mathbf{u}}_2 + \frac{\overline{\rho_1\mathbf{u}_1}}{\rho_0}.$$

The first equation (2.4) shows that the mean bulk velocity is solenoidal, that is, $\mathrm{div}\overline{\mathbf{u}}_2^M = 0$. It is related with the complex amplitudes $\overline{\mathbf{u}}_2^M = \overline{\mathbf{u}}_2 + \frac{\mathrm{Re}[\tilde{p}_1\tilde{\mathbf{u}}_1^*]}{2\rho_0 c_0^2}$. Projecting this equation on the x axis we obtain

$$\begin{aligned}\overline{u}_2^M &= \overline{u}_2(x,y) + \frac{\mathrm{Re}[\tilde{p}_1\tilde{u}_1^*]}{2\rho_0 c_0^2} = \overline{u}_2(x,y) + \frac{1}{2\rho_0 c_0^2}\\ &\times \mathrm{Re}\left[-(1-f)\frac{\rho_0 c_0^2}{i\omega}\frac{d\tilde{u}_0(x)}{dx}\tilde{u}_0^*(x)Y_x^*(y)\right]\\ &= \overline{u}_2(x,y) + V_0\,\mathrm{Re}\left[\frac{1}{4}i(1-f)G^*(x)Y_x^*(y)\right].\end{aligned} \tag{2.9}$$

Due to the solenoidality of the bulk velocity field, we can introduce the stream function ψ, such that

$$\overline{u}_2^M = \partial\psi/\partial y, \quad \overline{v}_2^M = -\partial\psi/\partial x. \tag{2.10}$$

Integrating Eq. (2.9) with respect to y we obtain the stream function in the form:

$$\psi(G,y) = \theta(G,y) + A_3(G)\frac{y^3}{y_0^3} + A_1(G)\frac{y}{y_0}, \tag{2.11}$$

where

$$\theta(G,y) = V_0\delta\,\mathrm{Re}\left[G(x)\{H_3(y) + iH_4(y)\} + \frac{1}{4}i(1-f)G^*(x)H_5(y)\right], \quad H_{3,4} = \delta^{-1}\int H_{1,2}dy, \quad H_5 = \delta^{-1}\int Y_x^*dy.$$

The coefficients of the even powers of y are taken to be zero, since ψ must be an odd function of y. From Eqs. (2.9) and (2.11) we obtain

$$A_3(x) = \frac{C_2(x)}{3}y_0^3, \quad A_1(x) = C_0(x)yy_0 + V_0\mathrm{Re}\left[\frac{1}{4}i(1-f)G^*(x)y\right]y_0,$$

$$H_3 = \frac{\sinh(2y/\delta) - \sin(2y/\delta)}{16|\cosh\beta y_0|^2} - \mathrm{Im}\frac{\sinh\beta y}{\beta\delta\cosh\beta y_0},$$

$$H_4 = f^*\frac{2\sinh\beta y - \beta y\cosh\beta y}{4\beta\delta\cosh\beta y_0} + \frac{i}{4\beta\delta}\frac{\sinh\beta^* y}{\cosh\beta^* y_0} - \frac{\sinh(2y/\delta) + i\sin(2y/\delta)}{16\beta\delta|\cosh\beta y_0|^2},$$

$$H_5 = \frac{y}{\delta} - \frac{i}{\beta\delta}\frac{\sinh\beta^* y}{\cosh\beta^* y_0}.$$

From Eqs. (2.9) and (2.10) we obtain an expression for the mean longitudinal bulk velocity

$$\overline{u}_2^M(G,y) = V(G,y) + V_0\mathrm{Re}\left[\frac{1}{4}i(1-f)G^*Y_x^*\right] + \frac{1}{y_0}\left[3A_3(G)\frac{y^2}{y_0^2} + A_1(G)\right].$$

Since $Y_x^*(y_0) = Y_x(y_0) = 0$, the unknown functions $A_1(G)$ and $A_3(G)$ are determined by the no-slip and impermeability conditions, respectively

$$\overline{u}_2^M(G, y_0) = 0: V(G, y_0) + \frac{3}{y_0} A_3(G) + \frac{1}{y_0} A_1(G) = 0,$$
$$\psi(G, y_0) = 0: \theta(G, y_0) + A_3(G) + A_1(G) = 0,$$

whence it follows that

$$\begin{cases} A_1(G) = -\frac{3}{2}\theta(G, y_0) + \frac{1}{2} y_0 V(G, y_0) \\ A_3(G) = \frac{1}{2}\theta(G, y_0) - \frac{1}{2} y_0 V(G, y_0). \end{cases}$$

The transverse component of the mean bulk velocity is determined by differentiating Eq. (2.11). Due to the linear dependence of θ, A_3, and A_1 on G we obtain

$$\overline{v}_2^M(G, y) = -\left(\theta(G', y) + A_3(G') \frac{y^3}{y_0^3} + A_1(G') \frac{y}{y_0} \right),$$

where $G'(x) = \dfrac{dG(x)}{dx}$.

3. RESULTS

In Fig. 2 the longitudinal and transverse components of the dimensionless first-approximation velocity (2.2) are presented on the left resonator boundary. In view of the symmetry of the velocity component u and the antisymmetry of the component v, we have plotted the profiles only for the upper half-plane of the resonator. The plots correspond to different stages of the period T with the step $T/8$. By virtue of the no-slip condition, the velocity at the vertical boundary is zero. It can be seen that the longitudinal component is constant (y-independent) almost everywhere on the left boundary but it varies strongly in the viscous boundary layer approaching zero on the upper and lower walls. As distinct from the longitudinal velocity component, the transverse component varies linearly in y almost everywhere, except from the viscous boundary layer. We note that these profiles correspond to the assumption on the one-dimensional nature of the pressure field, that is, $\partial p/\partial y = 0$.

In Fig. 3 we have presented the longitudinal and transverse components of the mean bulk velocity for the parameter values given in paper [10]. For the velocity scale we took the Rayleigh velocity $u_R = \dfrac{3}{16}\dfrac{U_m^2}{c_0}$, namely, the characteristic velocity of the acoustic streaming, where U_m is the maximum velocity of the acoustic streaming. The solid curves present the mean velocity profiles calculated in [10] for the resonator with an oscillating left boundary. The dots present the results calculated in [9] for an enclosure executing longitudinal oscillations. The dashed curves present the velocity profiles calculated for the resonator with an oscillating boundary. It can be seen that they are in good agreement with the results for the oscillating enclosure.

In Fig. 4 the streamlines of the acoustic streaming are presented in the form of four Rayleigh vortices and four Schlichting vortices. The similarity between the acoustic streaming occurring at horizontal enclosure oscillations (a) and at oscillations of the left resonator wall (b) is obvious. However, as distinct from the case of the oscillating enclosure, the acoustic streaming induced by the left wall oscillations is characterized by flows near the movable wall. In the case of the oscillating enclosure the centers of the Rayleigh and Schlichting vortices lie in the same cross-section, while in the case of the resonator with an oscillating wall these centers do not lie on the same line, the centers of the Schlichting vortices being displaced toward the side boundaries.

Although the excitation frequency ω in the solution obtained is arbitrary, it is conventional to consider the excitation on the lowest resonance frequency which will be denoted as ω_1. The method of determining ω_1 as a function of y_0/δ consists in the determination of an ω value, at which the longitudinal velocity component in the acoustic streaming is maximum at the center of the resonator. To estimate the complex amplitude of the velocity at the center of the resonator $|\tilde{u}_1(0,0)|$ we use the equation for the complex amplitude of the longitudinal velocity component of the in the first approximation: $\tilde{u}(x, y) =$

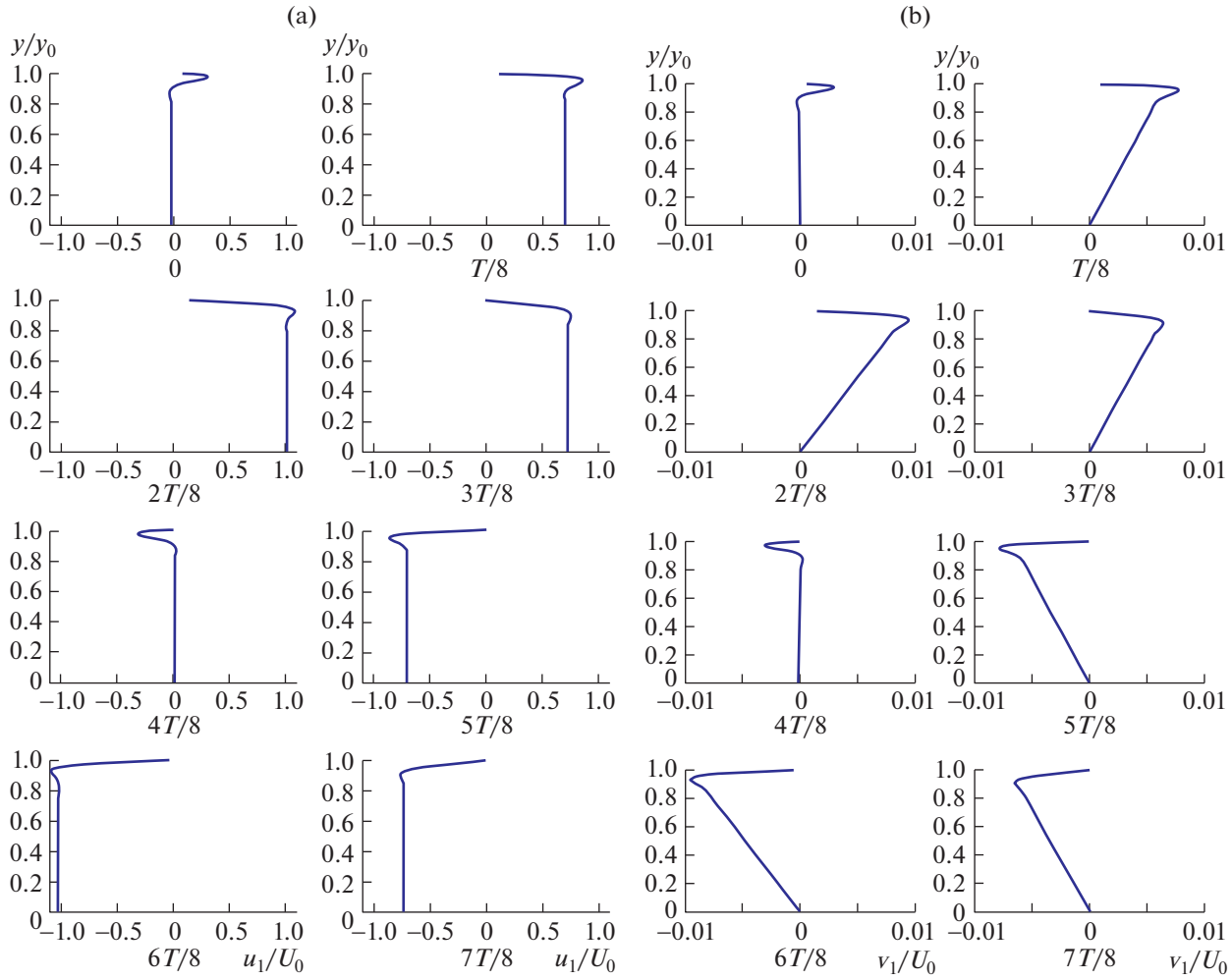

Fig. 2. Longitudinal (a) and transverse (b) components of the first-approximation velocity.

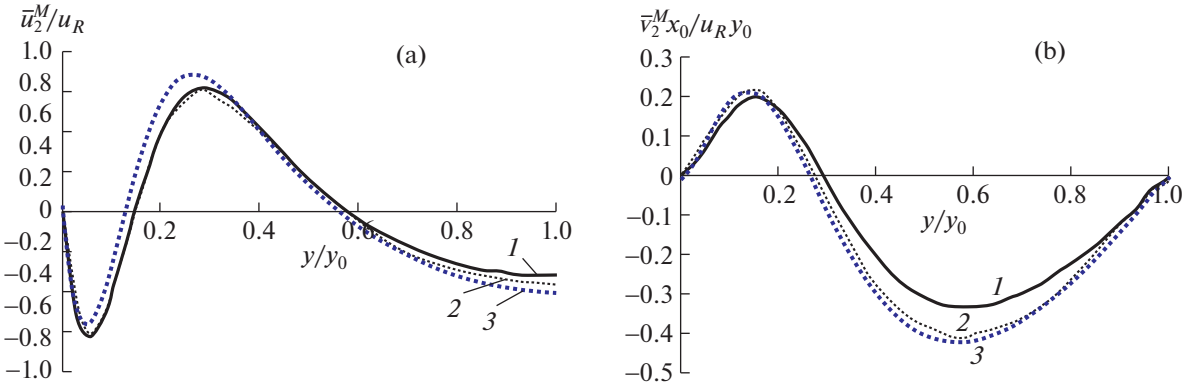

Fig. 3. Longitudinal (a) and transverse (b) components of the mean bulk velocity: *1*, results [10]; *2*, results [9]; and *3*, this study.

$\frac{0.5U_0}{1-f}\left(\frac{\cosh\alpha x}{\cosh\alpha x_0}-\frac{\sinh\alpha x}{\sinh\alpha x_0}\right)\left(1-\frac{\cosh\beta y}{\cosh\beta y_0}\right)$. Let $\omega_0 = \pi c_0/L$ be the fundamental resonance frequency. The values of ω_1/ω_0 thus obtained are presented in Fig. 5. At $\omega_1 = \omega_0$ the solution can be constructed as a function of x/x_0 and y/y_0, depending on the only parameter y_0/δ.

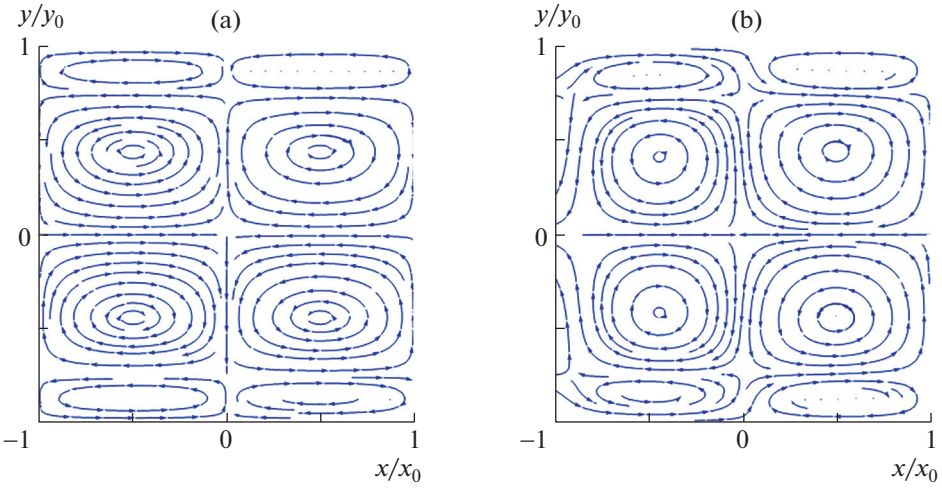

Fig. 4. Streamlines of the acoustic streaming; (a) oscillating enclosure and (b) oscillating left boundary.

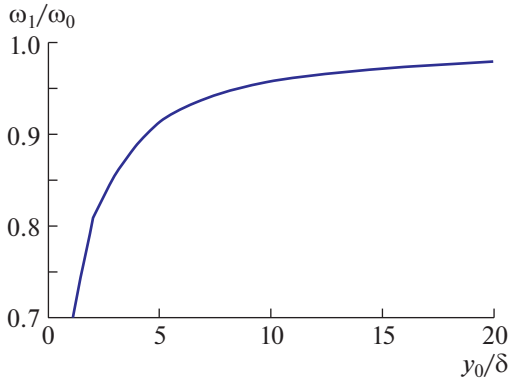

Fig. 5. Resonance frequency as a function of the channel width.

In Figs. 6a and 6b the first columns present the streamlines, the second columns are the distributions of the longitudinal velocity component in the section $x/x_0 = 0.5$ (in Fig. 6b the solid curves present the mean bulk velocity and the dashed curves present the mean velocity), and the third columns are the distributions of the transverse component of the mean bulk velocity in the section $x/x_0 = 0$. The similarity of the acoustic streamings occurring at horizontal enclosure oscillations (Fig. 6a) and at oscillations of the left resonator wall (Fig. 6b) is obvious, as well as a good agreement between the mean bulk velocities. In Fig. 6b the plots of the mean longitudinal and bulk velocities are presented in column 2. They are in good agreement, when the resonator width is greater than ten boundary layer thicknesses, $y_0 \geq 10\delta$. In the case in which the resonator width is smaller than six viscous boundary layer thicknesses, $y_0 < 6\delta$, the acoustic streaming is presented only by Schlichting vortices, while Rayleigh vortices are not formed.

SUMMARY

The approximate solution of the problem of an acoustic streaming in a rectangular resonator excited by the oscillations of its left boundary on the resonance frequency obtained in the study differs from the solution found in [9]. However, the comparison of the solutions shows that, except for a region near the oscillating wall, in particular within the enclosure and the resonator, Rayleigh and Schlichting vortices are generated. The condition of the applicability of the solution obtained is the smallness of the boundary layer thickness compared to the acoustic wave length, while the instantaneous velocity of gas particles is negligibly small compared with the speed of sound. The model used does not take account for the convec-

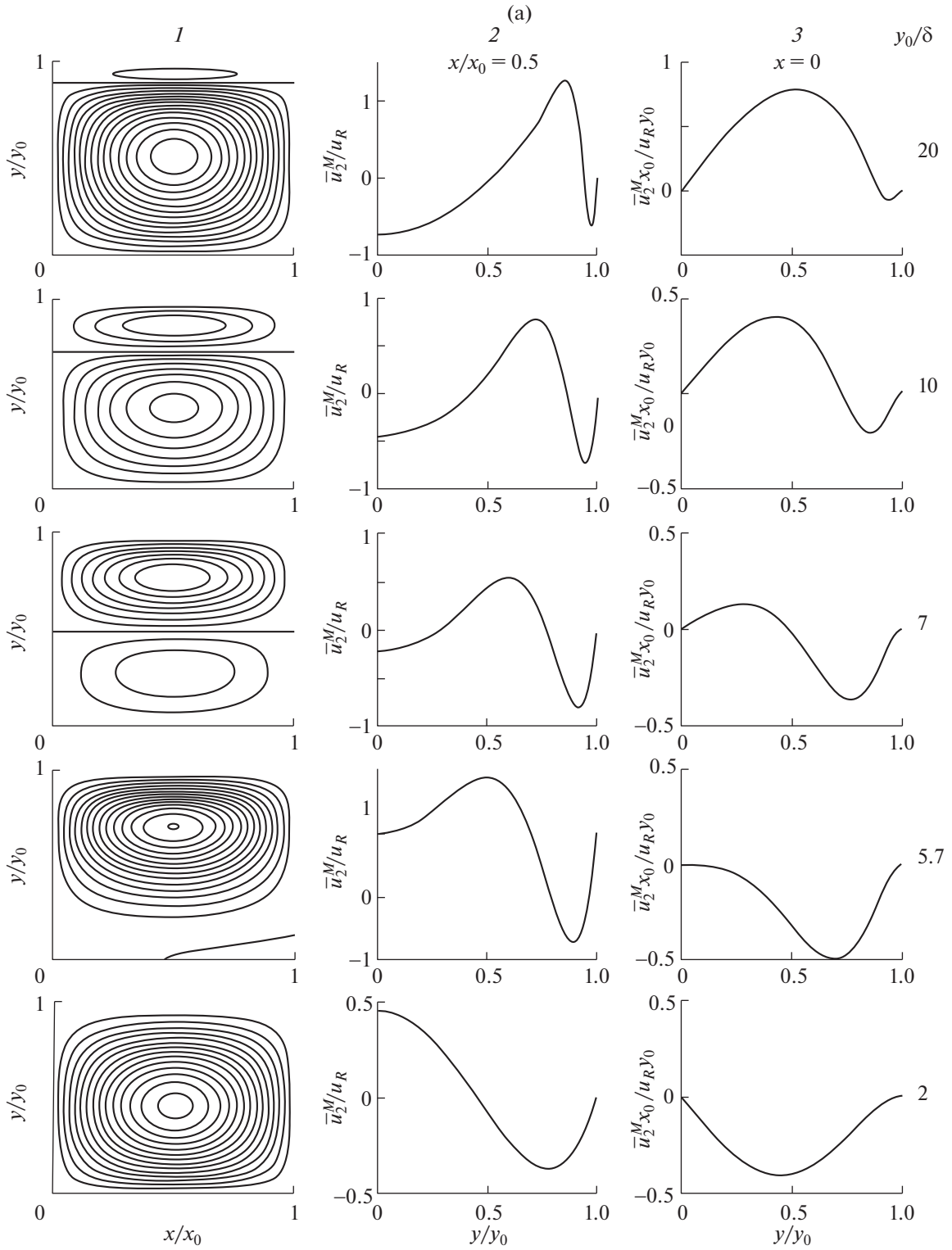

Fig. 6. Acoustic streaming parameters: (a) [9] and (b) results of this study; *1*, streamlines; *2*, distributions of the longitudinal velocity component in the section $x/x_0 = 0.5$ (solid and dashed curves relate to the mean bulk and mean velocities, respectively); and *3*, distributions of the transverse component of the mean bulk velocity in the section $x/x_0 = 0$.

tive acceleration of gas particles and the formation of a periodic shock wave at large oscillation amplitudes. The similarity between the acoustic streamings occurring at horizontal harmonic enclosure oscillations

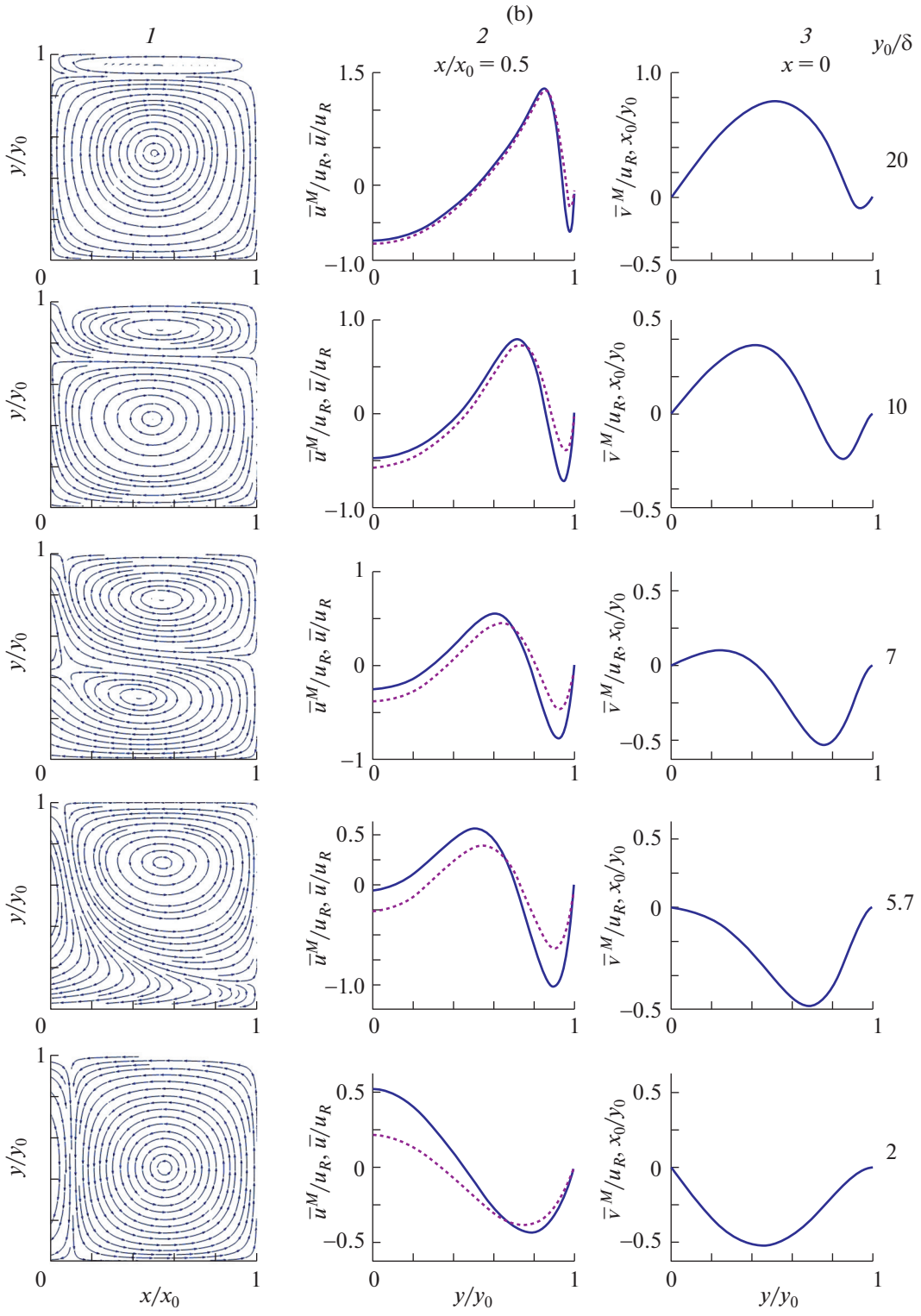

Fig. 6. (Contd.)

and at oscillations of the left resonator wall is established, which indicates that the way of standing wave generation has only a slight effect on the acoustic streaming patterns. In the case of the oscillating enclosure the centers of the Rayleigh and Schlichting vortices lie in the same cross-section, while in the case of the resonator with an oscillating boundary the centers of the Schlichting vortices are displaced toward the

side boundaries. A flow along the oscillating resonator wall is detected; it is due to the formulation of the boundary conditions.

FUNDING

The study was carried out with the financial support of the Russian Science Foundation (project no. 20-11-20070).

CONFLICT OF INTEREST

The authors declare that they have no conflicts of interest.

REFERENCES

1. Lord Rayleigh (Strutt, J.W.), On the circulation of air observed in Kundt's tubes, and on some allied acoustical problems, *Philos. Trans. Roy. Soc. London,* 1884, vol. 175, no. 3, pp. 1–21. https://doi.org/10.1098/rstl.1884.0002
2. Westervelt, P.J., The theory of steady rotational flow generated by a sound field, *J. Acoust. Soc. Am.,* 1953, vol. 25, pp. 60–67. https://doi.org/10.1121/1.1907009
3. Nyborg, W.L., Acoustic streaming, in *Physical Acoustics,* New York, 1965, vol. 2, part B, chap. 11, pp. 290–295. https://doi.org/10.1016/B978-0-12-395662-0.50015-1
4. Nyborg, W. L., Acoustic streaming, in *Nonlinear Acoustics,* San Diego, 1998, chap. 7, sec. 3.3.
5. Schlichting, H. and Gersten, K., *Boundary-Layer Theory,* New York: Springer, 2017. https://doi.org/10.1007/978-3-662-52919-5
6. Zarembo, L.K., Acoustic streaming, in *High-Intensity Ultrasonic Fields,* 1971, part III, pp. 135–199. https://doi.org/10.1007/978-1-4757-5408-7_3
7. Rudenko, O.V. and Soluyan, S.I., *Theoretical Foundations of Nonlinear Acoustics,* New York: Plenum, 1977, p. 206–210. https://doi.org/10.1002/jcu.1870060222
8. Gubaidullin, D.A., Osipov, P.P., and Nasyrov, R.R., Numerical simulation of Schlichting streaming induced by standing wave in rectangular enclosure, *J. Physics: Conf. Ser.,* 2014, vol. 567, p. 12017. https://doi.org/10.1088/1742-6596/567/1/012017
9. Hamilton, M.F., Ilinskii, Y.A., and Zabolotskaya, E.A., Acoustic streaming generated by standing waves in two-dimensional channels of arbitrary width, *J. Acoust. Soc. Am.,* 2003, vol. 113, pp. 153–160. https://doi.org/10.1121/1.1528928
10. Aktas, M.K. and Farouk, B., Numerical simulation of acoustic streaming generated by finite-amplitude resonant oscillations in an enclosure, *J. Acoust. Soc. Am.,* 2004, vol. 116, no. 5, pp. 2822–2831. https://doi.org/10.1121/1.1795332
11. Hamilton, M.F., Ilinskii, Y.A., and Zabolotskaya, E.A., Nonlinear two-dimensional model for thermoacoustic engines, *J. Acoust. Soc. Am.*, 2002, vol. 111, pp. 2076–2086. https://doi.org/10.1121/1.1467675
12. Zarembo, L.K. and Krasil'nikov, V.A., *Vvedenie v nelineinuyu akustiku* (Introduction in Nonlinear Acoustics), Moscow: Nauka, 1966.

Translated by M. Lebedev